ACS ENGINEERING Au
AN OPEN ACCESS JOURNAL OF THE AMERICAN CHEMICAL SOCIETY

pubs.acs.org/engineeringau
Review

Nozzle Innovations That Improve Capacity and Capabilities of Multimaterial Additive Manufacturing

Published as part of ACS Engineering Au virtual special issue "2023 Rising Stars in Chemical Engineering".

Patrick J. McCauley and Alexandra V. Bayles*

Cite This: *ACS Eng. Au* 2024, 4, 368−380
Read Online
ACCESS | Metrics & More | Article Recommendations

ABSTRACT: Multimaterial additive manufacturing incorporates multiple species within a single 3D-printed object to enhance its material properties and functionality. This technology could play a key role in distributed manufacturing. However, conventional layer-by-layer construction methods must operate at low volumetric throughputs to maintain fine feature resolution. One approach to overcome this challenge and increase production capacity is to structure multimaterial components in the printhead prior to deposition. Here we survey four classes of multimaterial nozzle innovations, nozzle arrays, coextruders, static mixers, and advective assemblers, designed for this purpose. Additionally, each design offers unique capabilities that provide benefits associated with accessible architectures, interfacial adhesion, material properties, and even living-cell viability. Accessing these benefits requires trade-offs, which may be mitigated with future investigation. Leveraging decades of research and development of multiphase extrusion equipment can help us engineer the next generation of 3D-printing nozzles and expand the capabilities and practical reach of multimaterial additive manufacturing.

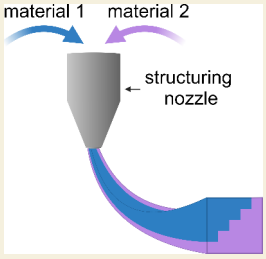

KEYWORDS: *multimaterial additive manufacturing, 3D printing, direct-ink writing, nozzle design, nozzle arrays, coextrusion, static mixing, advective assembly*

1. INTRODUCTION

Recent global supply chain disruptions have exposed the fragility of hypercentralized manufacturing networks. Delays in the production of an isolated component can stall the distribution of dependent products by months, causing substantial economic and societal loss.[1−3] Additive manufacturing (AM) provides the means for users to make certain custom components locally with minimal investment in capital equipment.[4−7] This technology has the potential to bridge production gaps and improve the resilience of supply chains provided that AM can meet the complex demands that are currently achieved using a suite of integrated production methods.

Compared with conventional manufacturing methods such as molding, machining, and forming, additive manufacturing has unique characteristics that have expedited its adoption. A single AM apparatus can be adapted for parts with varying geometric, material, and functional complexity without the need to retool.[8] Therefore, low-volume part production can be economically feasible.[9] Additionally, material waste is limited compared to subtractive manufacturing.[10] These benefits contributed to the widespread adoption of AM across diverse industries. The role of AM in manufacturing has rapidly evolved beyond rapid prototyping, and today it is used to fabricate many end-use parts.[11]

Growing demand for complex parts with advanced functionality has spurred the development of multimaterial additive manufacturing (MMAM). MMAM incorporates multiple species within a single 3D-printed object to produce unique physical, thermal, or electrical properties.[12−14] Some composite MMAM objects possess improved mechanical properties and enhanced functionality compared to their homogeneous counterparts.[15,16] For example, inks containing metallic or carbon fillers can be arranged to make parts directionally conductive and suitable for miniaturized electronics.[17,18] Inks containing living cells, biocompatible polymers, and sacrificial materials can be arranged to create scaffolds that direct cell proliferation and synthesize natural tissues.[19,20] Inks containing polycarbonate can be coextruded with low- or high-density poly(ethylene), making it possible to print with these ubiquitous plastics that are difficult to print alone.[21,22]

The rapidly growing and expansive field of AM has been the subject of many reviews. Several single-material AM techniques have been modified to incorporate multiple materials, including direct-ink writing, fused deposition modeling,

Received: January 4, 2024
Revised: April 15, 2024
Accepted: May 1, 2024
Published: May 13, 2024

material jetting, stereolithography, and digital light processing, among others.[16] Through this collection of techniques, virtually any combination of material classes—metals, ceramics, or polymers—can be processed.[23,24] Recent reviews have focused on MMAM developments for specific applications,[25−28] for specific materials or material properties,[29−31] and for specific AM techniques.[32−36]

One AM method that is particularly straightforward to adapt for multimaterial deposition is layer-by-layer direct ink writing (DIW). The simplest conceivable adjustment is to manually swap nozzles loaded with different materials during fabrication.[37,38] For example, consider 3D printing of a multilayered dielectric elastomer actuator[39−42] which requires alternating layers of elastomer and conductive electrode ink to be patterned over long ranges (Figure 1). In layer-by-layer

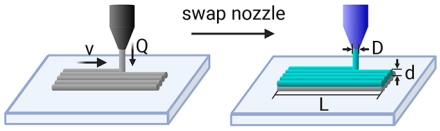

Figure 1. Simplest implementation of multimaterial additive manufacturing using direct ink writing. Here an electrode ink is loaded and deposited (left), and then the ink and nozzle are swapped to deposit a dielectric ink (right). Ink is deposited at a flow rate Q, while the nozzle rasters with a linear print speed v. The length of the part is L, and the smallest characteristic dimension, d, is the layer thickness, which is determined by the nozzle diameter D.

DIW, the electrode ink (gray ink in Figure 1) is loaded into a barrel or syringe and fed into a single conical-shaped nozzle, which is mounted on a 3D-printing arm that can raster in Cartesian coordinates. The nozzle containing the electrode ink traces a curvilinear print path while extruding the single-material filament, thus depositing the first layer. Then the electrode nozzle returns to the home base, and another nozzle containing the dielectric elastomer ink (cyan ink in Figure 1) is swapped onto the raster arm. The second nozzle traces the same print path, depositing the dielectric elastomer in a new layer on top of the electrode filament. The long-range structuring of the two contrasting inks extends the functionality of the MMAM part beyond that of single-material objects.

Although straightforward to implement, this nozzle-swapping approach has several drawbacks that must be addressed to produce high-quality multimaterial parts at appreciable scales. Exchanging nozzles increases manufacturing time (~5−10 s per nozzle swap in some implementations[20,43]) and potentially introduces defects. The flow of one material must be stopped and another started, and the raster arm must be carefully realigned to continue the print. Defects may also result from poor interfacial adhesion between contrasting layers, making the composite prone to fracture or delamination. Another challenge is the trade-off between resolution and the total build time. The resolution of the MMAM architecture inside a part is set by the diameter of the nozzle. For example, to achieve a d = 100 μm thick layer, a nozzle with a minimum diameter D = 100 μm is required, and in some cases the diameter of the final filament can significantly exceed the nozzle size due to die swelling ($d \approx 1.5D$; Table S1 in ref 44). Fine nozzles of this size must operate at low volumetric throughputs Q to avoid large pressure drops. In a circular pipe of diameter D, the pressure drop scales as D^{-4}. Thus, increasing the resolution (decreasing D) quickly generates impractical pressure drops that can be overcome only by decreasing the average extrusion speed. The low print speed combined with the small nozzle diameters of fine prints limits the total volumetric throughput. Large parts (e.g., 1 L) with very fine internal dimensions (e.g., $d \sim 100$ μm) will take several weeks to print with typical print speeds of $v \sim O(10)$ mm/s.[45,46]

Herein we review how some of these multimaterial additive manufacturing challenges have been addressed through innovations in nozzle engineering. Broad nozzle classes include parallel arrays, simple coextruders, miniaturized static mixers, and modular advective assemblers (Figure 2). In all cases,

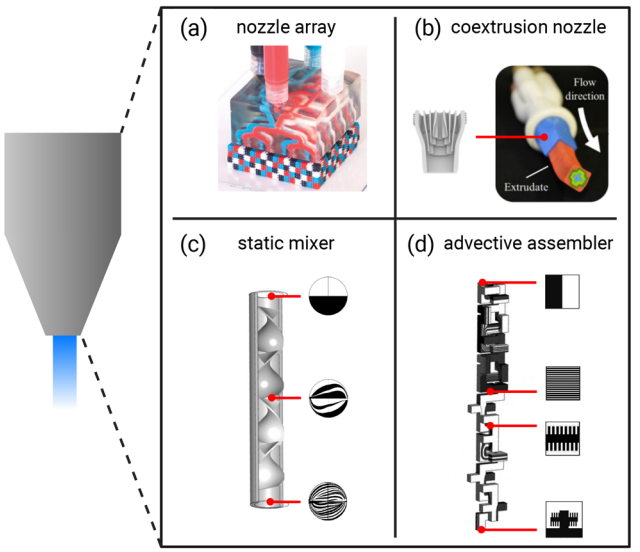

Figure 2. Innovative nozzle designs for producing multimaterial filaments. (a) Nozzle array which rapidly swaps between materials and deposits at several locations simultaneously. Reproduced with permission from ref 46. Copyright 2019 the authors of ref 46, under exclusive license to Springer Nature. (b) Coextruded filament with concentric layers of Play-Doh. Adapted from ref 48. CC BY 4.0. (c) Kenics static mixer with four elements that multiplies a two-layer stream into a stream of 32 alternating layers. Reproduced with permission from ref 49. Copyright 2011 Elsevier. (d) Serpentine advective assembler produces extrudates with fractal structures by combining, splitting, and rotating flow operations. Reproduced with permission from ref 50. Copyright 2013 Wiley-VCH.

feeding multiple inks into one mobile printhead structures composites prior to deposition and thus obviates the need to swap nozzles. We introduce the four classes through the lens of production capacity, i.e., the amount of material these nozzles can deposit in a given time, which has become increasingly prioritized as efforts to build distributed manufacturing networks have grown.

A survey of representative studies is provided in Table 1. The majority of the nozzles were not optimized to maximize throughput, but the operation values illustrate what is easily accessible and highlight the classes that have the greatest potential. These state-of-the-art multimaterial nozzles operate at similar capacities (v and Q) compared to single-gauge nozzles. For the nozzle array example, the flow rate reported is for only one outlet (Table 1). Therefore, the total capacity can be greatly amplified by increasing the number of outlets in the array. For the other nozzle classes, the minimum feature size d is no longer bound to the nozzle diameter and can be orders of

https://doi.org/10.1021/acsengineeringau.4c00001
ACS Eng. Au 2024, 4, 368−380

Table 1. Representative Printing Conditions Across Nozzle Classes

nozzle	D [μm]	d [μm]	v [mm/s]	Q [mL/min]	inks	function	ref
single-gauge	250	250	5	0.15[b]	silica sphere suspension	model colloidal ink	51
nozzle array[a]	250	250	20	0.4−0.8	silicones and others	actuation and soft robots	46
coextruder	1500	135	4	0.4	dielectric and conductive inks	strain sensor	52
coextruder	337	100	8	1	alginate, gelatin methacryloyl, and cells	bioprinting	53
coextruder	500	50	27	0.2[b]	poly(ethylene terephthalate glycol) and high-density poly(ethylene)	toughening and reduced filament warping	22
static mixer	230	230	10	6−30	silicones	graded materials	54
static mixer	1000	10	10[b]	0.003−5	alginate, gelatin methacryloyl, and cells	bioprinting	55
static mixer	1200	130	–	1.5	alginate, gelatin methacryloyl, and cells	bioprinting	56
forced assembler	2000 × 200	4	20	3	poly(vinyl alcohol) and multiwalled carbon nanotubes	strengthening and toughening	44
advective assembler	4000	333	1	1	poly(ethylene glycol) diacrylate and poly(acrylic acid) microgel	soft actuation	57
advective assembler	3000	130[b]	1	0.5	poly(ethylene glycol) diacrylate and poly(acrylic acid) microgel	support bath printing	58

[a]Values are for each outlet in the array. [b]The value was not reported and has been estimated from the print speed, flow rate, or filament dimensions.

magnitude smaller ($d/D \ll 1$). Nozzles that operate using the principles of layer multiplication (static mixers, forced assemblers, and advective assemblers) achieve the smallest d/D ratios. The differences in achievable resolution are due to the distinct operating principles of the four nozzle classes, described in detail in each of the sections.

After discussing how each nozzle class enhances production capacity, we then describe the ancillary capabilities and benefits that these nozzle innovations provide for the final printed parts. Each capability section primarily focuses on an emblematic challenge or opportunity in additive manufacturing that was addressed by the corresponding nozzle design. Nozzle arrays have been used to build soft robotics; coextrusion has been used to strengthen interfilament bonding; static mixers have been used to improve cell viability in extrusion-based bioprinting; and advective assembly has been used to sculpt hydrogel networks and program shape-responsive materials. Limitations and opportunities for future work are also briefly discussed in each section.

Finally, we provide an outlook for future studies that build upon the existing gains. Research in this area will contribute to a "New Direction for Chemical Engineering" identified in 2022 by the National Academies of Sciences, Engineering, and Medicine:[47] how can we apply principles of process intensification to advance distributed manufacturing? Achieving faster multimaterial printing with higher resolution will open new avenues for product development and manufacturing in multiple sectors which are enhanced by composite materials, including health care, electronic device fabrication, and food processing.[47] Widespread use of the technology will improve the resilience of supply chains and will empower small business owners and nonexpert users to enhance their internal prototyping processes and to produce sophisticated products with unique physical, thermal, and electrical properties, thereby democratizing manufacturing.

2. NOZZLE ARRAYS: PARALLELIZING EXTRUSION

Capacity

One approach for increasing MMAM production capacity is to parallelize extrusion using nozzle array printheads.[59] A nozzle array consists of multiple outlets positioned in a regular 2D pattern. A pioneering example of an MMAM nozzle array is shown in Figure 2a, where a printhead containing 16 outlets, each 200 μm in diameter, is crafted via stereolithography 3D printing.[46] These outlets function differently than in typical nozzle-swapping instrumentation, where each nozzle is associated with a single ink formulation.[20,43] Instead, in the nozzle array, each outlet dynamically swaps between all ink formulations. In Figure 2a, four different inks are fed into the array and deposited simultaneously from each outlet. Material feeds are diverted to each outlet using a microfluidic printhead that is designed to swap between inks with minimal lag time by toggling the inlet feed rate or pressure through connected channels.[60] Other approaches have been explored to swap materials deposited by a single nozzle such as by bundling capillaries that feed separate materials[61] or by using mixing elements (section 4). These other examples also reduce overall build time but do not achieve the same throughput gains realized by the microfluidics-based nozzle array.

Since all of the outlets extrude simultaneously and occupy separate print areas, the nozzle array can achieve a higher total volumetric throughput than the equivalent single nozzle. Printed parts are built up voxel-by-voxel rather than in the layer-by-layer manner required by conventional direct ink writing. The time required to print an MMAM object of length L scales as L^3 using a single nozzle versus L using a 2D nozzle array.[46] Additionally, the array design addresses the limitations of nozzle swapping since the raster arm does not have to rehome every material, resolving nozzle alignment problems and saving time. Thus, extruding multiple materials from arrays parallelizes production and reduces the overall build time.

Capabilities

Nozzle arrays are well-suited to manufacture parts that derive functionality from periodic structures. Contrast between material properties can be used to direct actuation. A classical example is when materials, commonly metals, with ordered regions of contrasting thermal expansion coefficients macroscopically bend in response to temperature changes.[62] Shape responsiveness incorporated into the final part adds time dependence and another dimension to 3D printing and is thus frequently referred to as 4D printing.[63] Using a nozzle array, Skylar-Scott et al.[46] simultaneously deposited silicones with contrasting elasticity to produce 16 pneumatic actuators, which were the feet of a soft-robotic walker. Under a cycling vacuum,

https://doi.org/10.1021/acsengineeringau.4c00001
ACS Eng. Au 2024, 4, 368−380

these actuators buckled and unbuckled to propel the walker forward at up to 1 cm s^{-1} while carrying a load of up to 200 g. In this example, printing the soft robot with an array reduces build time compared to using a single nozzle, and importantly, the nozzle array is straightforward to scale up to simultaneously produce an even greater number of actuators if desired.

Although the parts produced by nozzle arrays are functional, one drawback is that the multimaterial architectures are spatially constrained. Since the distinct materials are deposited simultaneously at the same rate from all outlets, the resultant part can have only periodic structures that are multiples of the original 2D array. Printed topologies are also generally restricted to Cartesian coordinates, although recent progress has been made using arrays that rotate as they extrude twisted, touching filaments.[64] The voxel resolution places additional constraints on attainable architectures; all patterns must be multiples of the voxel size, here between 300 μm and 2 mm, which tends to be coarser than the outlet diameter. To circumvent this limitation and achieve finer resolution, heterogeneous flows can be patterned, multiplied, and extruded from a single outlet as described in the following three sections.

3. COEXTRUSION NOZZLES: PATTERNING FILAMENTS

Capacity

Whereas a nozzle array extrudes only one material from each outlet at a time, a coextrusion nozzle extrudes multiple materials from one outlet simultaneously. The field of coextrusion was developed well before additive manufacturing and has been intensified for the manufacturing of a variety of commercial products. Many mature coextrusion processes involve multilayer polymer films and sheets with enhanced properties, much like polymeric MMAM.[65,66] This established technology has been integrated into additive manufacturing processes to extrude high-fidelity multimaterial filaments with $O(10)-O(100)$ μm internal architectures.[52,67,68] These are the length scales typically encountered in microfluidics, and therefore, the principles of microfluidic laminar, multimaterial, and multiphase flows are frequently leveraged to design coextrusion nozzles.[69,70] The laminar flows within these nozzles are aligned along the flow direction, with only diffusive mixing between heterogeneous regions. Therefore, structured flows maintain high fidelity; subdiameter resolutions are achieved using print speeds on the order of 10 mm/s (Table 1), allowing users to maintain volumetric throughput while improving resolution.

Capabilities

The fine structures produced by MMAM coextrusion impart various electrical, thermal, or mechanical functionalities to the printed parts. One of the key advantages of coextrusion is that a continuous material phase is produced, which is critical for the performance of conductors. In one example, a radially symmetric multicore−shell filament was extruded using two inks via an annular die, producing soft strain sensors.[52] In a different case, coextrusion was used to create carbon-fiber-reinforced nylon composites with a continuous filler phase, which exhibited greatly enhanced thermal conductivity compared to that with a discontinuous filler.[71] Coextrusion nozzles have also been used frequently in extrusion-based bioprinting, particularly for improving the mechanical properties of filaments[53,72] or for creating hollow structures that mimic vascular tissue.[73−75]

A key challenge in additive manufacturing addressed by core−shell coextrusion is interlayer adhesion deficiencies,[22,67,76] which are most frequently encountered in fused-deposition modeling. Fused-deposition modeling, a form of 3D printing where molten thermoplastic filaments are deposited, is ideal for creating highly customizable prototypes at a low cost. However, the parts produced often lack in quality sufficient for end-use applications.[77,78] Critically, the mechanical properties suffer because of voids and poor adhesion between the deposited layers. These problems arise because of competing cooling requirements after filament deposition; rapid cooling of the filament from its molten state prevents deformation of the printed object, but slow cooling promotes coalescence and interdiffusion with adjacent filaments. Weak interfilament bonds generate significant anisotropy where the part's strength along the build direction (perpendicular to the printer platform) is 40−50% lower than that along the other directions.[79]

Interfilament bonding can be improved by optimizing printing parameters—deposition speed, nozzle temperature, raster angle, and build orientation[78]—or by using multiple materials with complementary properties. Often coextruded filaments are produced first and then re-extruded through a standard printing nozzle,[21,67,76] but recently these operations have been combined directly into the nozzle using an innovative coextrusion die.[22] Peng et al.[67] demonstrated that coextruded core−shell filaments could produce MMAM objects with enhanced impact resistance. The core material was a polycarbonate, a stiff high glass transition temperature (T_g) polymer that reinforced the printed shape, and the shell material was a poly(ethylene-*co*-methacrylic acid), a low T_g polymer that promoted interdiffusion of adjacent filaments. Because of these complementary material properties, this composite system improved interfacial bonding without sacrificing the shape quality. Improved printability and mechanical properties have been demonstrated using different polymers such as low- or high-density poly(ethylene) in the shell,[21,22] widely used consumer plastics that are difficult to 3D-print alone. In one instance, coextruded filaments enhanced the tensile strength and impact toughness severalfold along the build direction, addressing a key weakness in 3D-printed polymer parts.[80]

These examples highlight how simple core−shell or side-by-side architectures can enhance the properties of the filament and consequently improve the overall part. However, creating more complex architectures and scaling to larger filament sizes and higher throughputs (while still obtaining micrometer-scale structures) require more complex coextrusion nozzle designs. Recently, a computational design synthesis framework was developed to expedite the creation of coextrusion nozzles which structure various inlet flows into complex cross-section patterns (Figure 2b).[48] This automated approach streamlines an otherwise laborious process of computer-aided design and computational flow dynamics validation. However, the resulting nozzles are highly complex and have only been demonstrated to create structures with $d \sim O(1)$ mm. Smaller-length-scale structures are likely inaccessible because any structure in the filament is constrained by the internal nozzle dimensions (e.g., the thickness of the various internal sheaths and vanes). A class of nozzles is required that can create structures not limited by the dimensions of the nozzle itself.

https://doi.org/10.1021/acsengineeringau.4c00001
ACS Eng. Au 2024, 4, 368−380

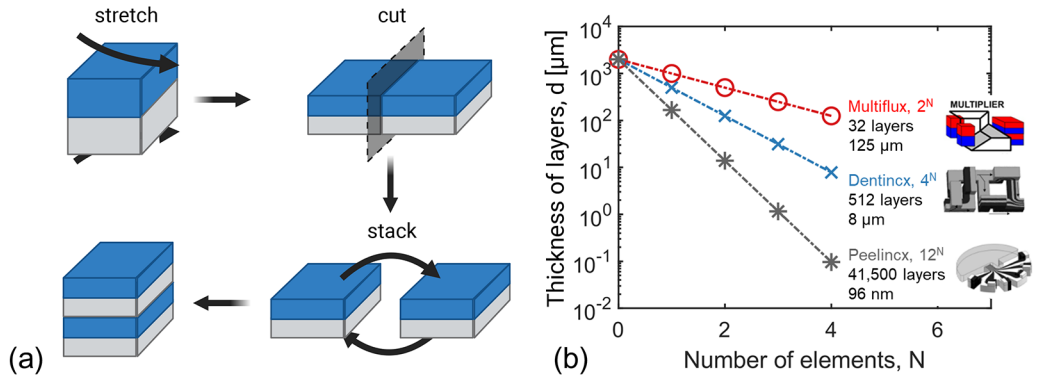

Figure 3. (a) Baker's transformation multiplying two stacked layers into four. The layers are stretched, cut, and stacked to double the number of layers. The total dimensions of the layer assembly before and after the transformation are equal. (b) Reduction of layer thickness d with an increasing number of multiplying elements in three unique devices: the Multiflux,[90] Dentincx,[91] and Peelincx mixer elements.[91] These mixers multiply the number of layers by factors of 2, 4, and 12, respectively. Using only a handful of elements, submicron layer thicknesses are accessible. The inset images are reproduced with permission from refs 90 and 91. Copyright 2010 and 2011, respectively, Wiley-VCH.

Fortunately, there are high-throughput devices that meet these challenges that have been refined over decades in processing industries and may be readily adopted and modified for MMAM: static mixers.

4. STATIC MIXERS AND FORCED ASSEMBLY: MULTIPLYING LAYERS

Capacity

Static or "motionless" mixers are processing tools designed to blend disparate materials by progressive layer multiplication.[49,81,82] In low Reynolds number flows, like those often encountered in 3D-printing nozzles, passive mixing occurs only through diffusion, and therefore, maximizing interfacial area is critical to adequately blend materials. Most commonly, these devices consist of a circular pipe containing internal baffles such as the helical fins of the so-called "Kenics" mixer in Figure 2c. Two fluids are driven by an applied pressure into the baffled pipe, and as the dual feed advects along the series of baffles, the layers double after each mixing element following a mathematical principle known as the baker's transformation (Figure 3).[49,83] The thickness of the multiplied layer rapidly decreases at a rate of 2^{-n}, where n is the number of baffles in series, and eventually, the fluid homogenizes. This chaotic advection process is particularly efficient at blending high-viscosity fluids,[84,85] much like some of the materials used in MMAM.

One valuable feature of static mixers is that they can be scaled up to several feet in diameter while maintaining high flow speeds.[86] Static mixers can also be scaled down to millimeter and micrometer scales.[87−89] For example, the Kenics mixer (Figure 2c) is commonly sold at hardware stores as a millimeter-scale adapter for blending two-component epoxy adhesives. The ability to adapt equipment across multiple length scales is appealing for additive manufacturing since nozzles can be designed for fine or large-diameter filaments while exploiting the same principles. The principles of predictable layer multiplication are useful not only for efficiently increasing surface area to blend materials at scale but also for creating structured, irregular material regions. To achieve uniform structuring, static mixing extruders must be designed and optimized with different goals in mind.

The field of forced assembly exploits static mixing principles to structure rather than to blend. Using forced assemblers, high-resolution layered architectures much smaller than the nozzle diameter are obtainable ($d \ll D$, Figure 1). For example, a simple Kenics static mixer (Figure 2c) was incorporated into a DIW nozzle to perform forced assembly.[55] This process, coined "continuous chaotic printing", produced 2 mm diameter filaments that contained layers of thickness $d \sim 10-100$ μm. Furthermore, feeding this layer multiplication into an electrospinner created structural features with nanoscale resolution (~150 nm).

Some static mixers have been designed specifically for forced assembly in polymer processing—particularly for multilayer film fabrication[92−94]—which could also be useful for MMAM. These mixer devices multiply layers using the principles of the baker's transformation[95−97] and when placed in series produce thin-layered structures. Three notable devices are the Multiflux, Dentincx, and Peelincx mixers (Figure 3b).[90,91] These mixers were designed to improve layer uniformity and multiplying efficiency (see scalings in Figure 3b) compared to standard static mixers like the Kenics mixer.[94] With only four mixing elements, hundreds or thousands of micrometer- or nanometer-scale thickness layers can be fabricated (Figure 3b). Also, this extrusion can be performed at a sufficiently high throughput to produce commercially viable products, including gas barrier[98−101] and photonic films.[102,103] In these cases, the multimaterial products are manufactured directly by extruding layered stacks from a forced assembly die, not by incrementally building them on a rastering 3D printer.

A layer-multiplying mixer was incorporated into an MMAM nozzle to generate layered structures with excellent resolution while maintaining throughput comparable to that of other nozzle designs (forced assembler in Table 1). Ravichandran et al.[44] incorporated Multiflux-type layer-multiplying elements into a printhead nozzle to produce rectangular filaments with alternating layers of a poly(vinyl alcohol) polymer solution and carbon nanotube suspension. In this process, which was called multiphase direct ink writing (MDIW), these materials were coextruded through one to seven multiplying elements to compare the composite material properties between structures of varying layer number and thickness over a wide range (4−512 layers of 500−4 μm). The plug-and-play multiplying elements permit studies of this kind to be performed quickly and without tooling a range of different nozzles.

https://doi.org/10.1021/acsengineeringau.4c00001
ACS Eng. Au 2024, 4, 368−380

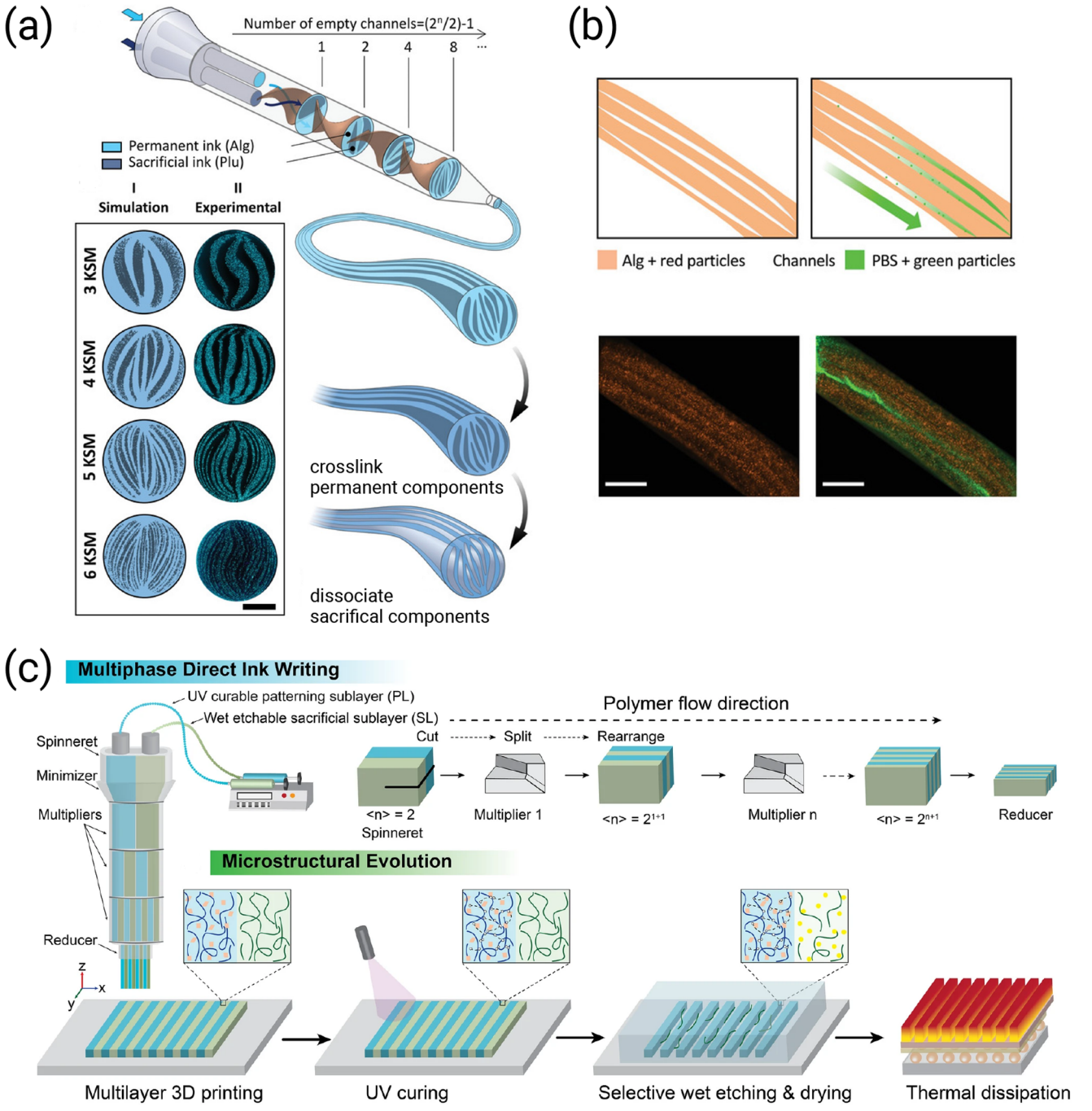

Figure 4. (a) Creation of alginate filaments with hollow channels using a Kenics static mixer. The number of channels increases with the number of mixer elements *n*. These channels are visualized (b) with an infiltrating phosphate-buffered saline (PBS) solution seeded with green fluorescent particles. Reproduced with permission from ref 114. Copyright 2022 Wiley-VCH. (c) Layer-multiplying nozzle to produce filaments with alternating layers of thickness $d \sim 100\ \mu m$. UV curing of a permanent epoxy followed by wet etching of sacrificial poly(ethylenimine) ink yields a micropatterned ridged surface. Reproduced with permission from ref 115. Copyright 2023 the authors of ref 115, under exclusive license to Springer Nature Switzerland AG.

Capabilities

Static mixers have the potential to create fine-resolution structures with unique capabilities, but using them to blend has also been fruitful in several state-of-the-art MMAM applications. Due to their efficient blending, static mixers have been adopted into nozzle designs to print multicomponent materials that are conventionally challenging to extrude and to create MMAM parts with gradient properties.[29] For example, static mixers have been incorporated into nozzles to print two-part epoxy resins, where mixing the resins just before deposition improves extrudability without compromising shape quality.[104] Using custom static mixer designs, very high viscosity (~81000 mPa at a shear rate of 1 s^{-1}) resins can be thoroughly mixed and extruded into parts.[105]

If the feed ratio into the static mixer is continuously varied, smooth gradients in material properties can be gener-

https://doi.org/10.1021/acsengineeringau.4c00001
ACS Eng. Au 2024, 4, 368−380

ated,[29,106−108] which mimic the property gradients found in a wide range of biological structures such as bamboo, bones, and tendons.[29,109,110] In these biological materials, variations between soft and stiff regions impart both high strength and toughness, which are typically orthogonal material properties. Graded materials can also increase resistance to interfacial failure between regions with disparate properties,[111] which is a key problem in artificial implants.[112] To fully realize these benefits, next-generation nozzles have been developed to handle inks with more diverse properties, to reduce mixing volume and allow rapid composition changes, and to reduce shear stresses detrimental in bioprinting.[54,105,113] Additionally, with careful planning of the print path and feed rates, gradient properties can be created in three dimensions throughout the printed part.[111]

When used to blend, static mixers are effective for making biomimetic gradient materials, but static mixers have also been used as structuring nozzles to address key limitations in extrusion-based bioprinting.[55,56] Accessing high-resolution features while maintaining cell viability is difficult to achieve by using standard single-gauge nozzles in extrusion-based bioprinting. Decreasing the nozzle diameter amplifies the shear stresses imposed on the cells during extrusion, reducing cell viability.[73,116,117] Consequently, filament resolution is at minimum $\gtrsim$100 μm and typically between 150 and 300 μm.[118,119] This resolution limit, constrained by the nozzle diameter, can be exceeded by structuring the filament upstream using the principles of static mixing and forced assembly. This concept was demonstrated in recent works where muscle-like tissue constructs were created by coextrusion of two hydrogels through a Kenics static mixer (Figure 4a,b).[55,56,114,120] In one of these works,[56] a static mixer with three elements was incorporated into the nozzle to form eight intercalated layers of myoblast-laden and cell-free barrier hydrogels with thicknesses $d \sim 130$ μm. This fine resolution was achieved while maintaining excellent postprinting cell viability because the total filament radius was relatively large (~1.2 mm), leading to lower shear stresses and cell damage during printing.

Follow-up work has expanded the capabilities afforded by the use of static mixers in bioprinting. Hollow microchannels were formed by replacing the cell-free barrier hydrogel with a sacrificial ink (Pluronic F127), which is removed after printing (Figure 4a,b). This process is often called "vascularization" in the field of bioprinting.[20,74,121] Consequently, cell viability near the center of the filaments improved,[114] as vascularization permits the transport of cell waste and growth media, which are necessary functions to maintain viability that are limited in tissues with thickness exceeding $\gtrsim$100−200 μm.[122] Recently, Kenics static mixers have been incorporated into more complex extrusion systems allowing several material feeds and variations along the filament length.[123]

One limitation of MMAM nozzles that utilize commercial static mixers is that the architectures produced are spatially constrained to the streamline distribution within the baffles. The characteristic dimensions of these patterns tend to be finer than those produced by voxelated 3D-printing arrays or standard coextrusion nozzles, but the geometric complexity of the pattern is significantly more difficult to customize. As illustrated in Figure 4a, the Kenics baffles produce layers that have fairly uniform thicknesses, but those layers warp across the circular cross-section. The streamline distribution is effective for mixing two fluids and useful for structuring in bioprinting, but the distortions can produce catastrophic defects in certain MMAM applications. For example, the stacked dielectric actuator depicted in Figure 1 would short if any of the conductive layers were touched.

In applications that require precise organization, forced assembly offers solutions. The MDIW (Figure 4c) nozzle extrudes stacks of even, parallel layers orders of magnitude thinner than the die's outlet diameter, which impart additional capabilities to printed parts. These fine-layered filaments have been formed into parts that are both magnetically and thermally responsive.[124,125] Thermoplastic poly(urethane) (TPU) was mixed with iron oxide nanoparticles in one ink to impart a magnetic field response and mixed with poly(caprolactone) in the other ink to impart a thermal response. Therefore, these parts had both shape memory, unrolling or unfolding in response to heating, and anisotropic magnetization properties, orienting macroscopically in different directions in response to an applied magnetic field. The orientation of the layers was important for both properties, demonstrating how these layered architectures can provide anisotropic material properties to parts. Furthermore, the exceptional control of layer uniformity and size can be leveraged for micropatterning (Figure 4c). After printing with the MDIW nozzle and subsequently etching away sacrificial material, microgrooves of epoxy laden with boron nitride particles were fabricated with a resolution between 50−200 μm.[115] Micropatterning is achieved through a variety of techniques, most commonly lithography or vapor deposition.[126] However, this 3D-printing approach offers a simple, scalable, and cost-effective alternative.

These examples demonstrate that rapidly ordering multiple materials at single-digit micrometer length scales has the potential to greatly accelerate MMAM production, provided that the structures extruded by nozzles are useful in the 3D-printed part. To move beyond layered stacks and customize MMAM architectures for specific applications, principles of the nascent field of advective assembly can be leveraged to intensify production patterns of even greater complexity.

5. ADVECTIVE ASSEMBLY: MULTIPLYING DESIGNER PATTERNS

Capacity

Advective assembly (AA) nozzles consist of networks of closed millifluidic channels connected by splitting, rotating, and recombining fluidic junctions.[57,127] Like the baffles in static mixers, AA junctions are repeated in series to multiply patterns and shrink their characteristic dimension. Unlike the baffles in static mixers, the junctions are organized in particular sequences to distribute coflowing materials in a hierarchical structure rather than in an even distribution.

The concept of building modular sequences from junction building blocks was first introduced in pioneering work by Neerincx and Meijer,[50] who showed that dendritic tree structures can be assembled by carefully introducing rotation junctions into a forced-assembly layer multiplier. The extruded architectures have five levels of hierarchy (Figure 2d) with nominal length scales of 5000, 1830, 1200, 580, and 140 μm.[50] Due to the fractal-like appearance of the multiplied pattern, this approach was described as "fractal processing".[94,128] Here the term "advective assembly" is preferred since the same junctions can be combined to produce arbitrary patterns that do not necessarily qualify mathematically as fractals.[57,127] The

https://doi.org/10.1021/acsengineeringau.4c00001
ACS Eng. Au 2024, 4, 368−380

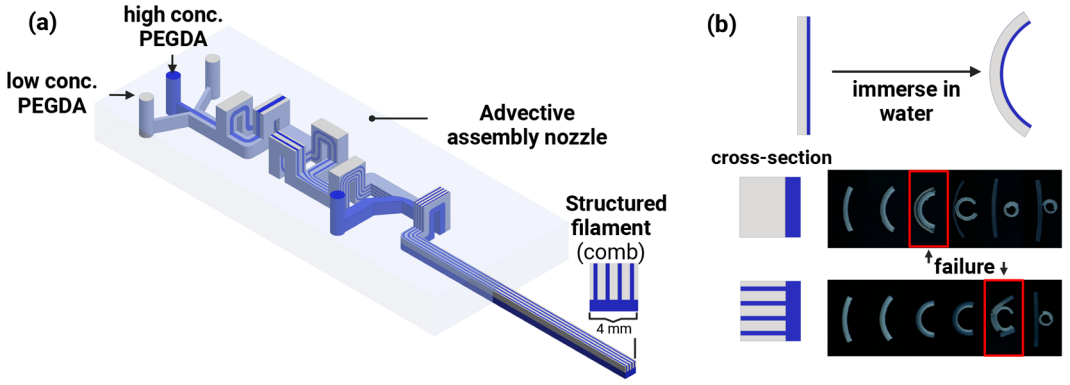

Figure 5. (a) Serpentine assembler that structures low- and high-concentration PEGDA solutions into a comb architecture. (b) Swelling of PEDGA soft actuators with high concentration (blue) and low concentration (gray) regions. Changing the filament architecture from a bilayer to a comb architecture extends the achievable bending curvature before failure and delamination. Reproduced from ref 57. Copyright 2022 American Chemical Society.

"advective" descriptor also harkens back to the chaotic advection mechanism of efficient streamline multiplication.

The fractal pattern produced by the advective assembler in Figure 2d is reminiscent of the voxel-by-voxel pattern achieved by the nozzle arrays. However, to produce the same small features using the nozzle array, outlets an order of magnitude smaller in diameter would be required and would have to be operated at an appropriately low volumetric throughput. In contrast, the external diameter D of a patterned filament extruded by the advective assembler can be relatively large (4 mm × 4 mm square cross-section in ref 57), and therefore, these complex fractal patterns can be made without compromising throughput.

The ability to continuously and scalably build multimaterial architectures with flow is of great interest in manufacturing industries outside of MMAM. Drawing from implementations in other industries may accelerate the design of high-capacity AA printing nozzles. Recent developments in AA have shown that the devices are particularly efficient at producing monodisperse emulsions from oil and water feeds that have too high a viscosity mismatch to be emulsified via conventional droplet schemes.[129] There, feeds of high-molecular-weight poly(isobutylene) (PIB) and water were fed into an AA device, which multiplied the oil−water interfacial area as the stream passed through the wagon-wheel junction sequence. Once the characteristic thickness of the layers thinned sufficiently, the layers broke into droplets and formed a high ($\eta_{oil}/\eta_{water} = 10^4$) viscosity mixture. The continuous processing scheme has the potential to be scaled commercially[130,131] and adapted for other products such as multicomponent food dispersions (e.g., chocolate, wheat dough, and melted cheese).[132]

The utility of advective assemblers for MMAM is just starting to be explored. The first demonstration of AA used the nozzle in Figure 5 to produce soft hydrogel actuators. There, low- and high-concentration poly(ethylene glycol) diacrylate (PEGDA) precursors were fed at total volumetric throughputs of 1 mL/min and structured into a comblike architecture with characteristic feature sizes of 300 μm. Compared to other MMAM benchmarks, this volumetric throughput is 1 order of magnitude greater than that of layer-by-layer methods;[45,57] however, some distortion of the comb pattern is observed. Elucidating the trade-off between filament pattern fidelity and throughput for particular material rheologies is an active area of investigation.

Capabilities

Preliminary studies using advective assemblers as MMAM printing nozzles demonstrate that they address some grand challenges in MMAM. Namely, they have been shown to provide useful functionality (e.g., actuation), provide access to geometrically complex architectures that are not constrained to Cartesian coordinates, and improve printed parts' mechanical properties.

In the example shown in Figure 5, dilute and concentrated solutions of PEGDA were fed through a serpentine assembler to create filaments with regions of low and high cross-linking density patterned into a comb architecture. When the internally templated filaments are immersed in water, the low-cross-linking-density portion swells more than the high-cross-linking-density portion, causing the straight filament to bend into an arc with a curvature programmed by feed flow rates. The macroscopic shape of the flow-templated hydrogel filament is dictated by the translation of the AA printhead. The AA approach can be used to fabricate actuating claws that open and close (a canonical 4D printing demonstration[63,133]) in a single printing pass. Moreover, the AA approach can be used to construct soft actuators in a Möbius strip shape, where the cross-linking density twists smoothly along the circumference of the printed part, which would be impractical to construct via conventional layer-by-layer MMAM. Recent work uses AA nozzles with support baths to build helical structures and expand the topological design space beyond the Cartesian plane.[58]

Assembling the multimaterial architectures inside the nozzle improves interfacial adhesion. While the miscible materials flow through the nozzle, the species have a finite time to interdiffuse, creating interfaces between contrasting regions that are diffuse rather than sharp. Curing the multimaterial filaments at once also improves bonding between the regions compared to sequential layer-by-layer construction. Delamination measurements[57] also suggest that the comb patterns fabricated by advective assemblers can undergo larger deformation strains compared to simple bilayers fabricated by coextrusion nozzles. The comb teeth are akin to Velcro bridging the two regions of variable cross-linking density.

Advective assemblers grant access to high-resolution, geometrically complex architectures that are inaccessible using the other nozzle classes, provided that specific rheological constraints are met. To maintain high feature

https://doi.org/10.1021/acsengineeringau.4c00001
ACS Eng. Au 2024, 4, 368−380

fidelity, all of the materials fed into the assemblers must have similar rheology.[44,57] Substantial viscosity differences at process shear rates can cause viscous encapsulation, a phenomenon where the less viscous fluid migrates toward the wall of the flow geometry.[134,135] If the materials have viscoelasticity, distortions can also arise because of elastic instabilities and secondary flows induced during stretching and rotating operations.[50,94,136] These challenges are partially addressed through careful design to remove device asymmetry,[137,138] but another approach is to select ink formulations with minimal viscoelasticity such as granular material (the approach applied in Figure 5). These elastic and mismatched rheology effects can impact all nozzle classes that coextrude material, but distortions are more prevalent in forced and advective assemblers due to the high layer uniformity and complex nozzle designs and flow paths.

Architectures with substantial geometric complexity, such as fractal structures (Figure 2d), require many flow operations to assemble. These flow operations increase the length of the nozzle, increasing pressure drop and residence time of materials in the device. Residence time is important to consider when high pattern fidelity is required, as longer residence times will increase interdiffusion and blend features.[57] However, this effect could be beneficial in applications requiring greater interfacial adhesion. Another consideration is the design and fabrication of complex advective assemblers. Fortunately, the fabrication method is robust, and virtually any set of flow operations can be linked together to produce a desired pattern. Designing an advective assembler to produce that pattern is more challenging, but recent work has presented a Boolean logic framework to convert flow operations into circuit operations, allowing for rapid design of "flow circuits" to build complex filament architectures.[139]

6. OUTLOOK

Innovations in nozzle design increase production capacity without sacrificing feature resolution and improve multimaterial parts' capabilities because a portion of structuring occurs upstream of the printbed. Preassembling architectures before deposition is akin to prefabricating modular houses in a centralized location before distribution across construction sites. Build times can be significantly reduced through parallelization, and greater geometric complexity, resolution, and functionality in the final product are possible. Systematic studies are needed to assess maximal throughput gains. Computational fluid dynamics tools will be essential in these studies since they can cover a wide range of operating conditions and be pushed to extremes without requiring immense volumes of material or extrusion forces that are difficult to generate in the laboratory.

The distinct nozzle classes surveyed here (nozzle arrays, coextruders, static mixers, and advective assemblers) provide unique combinations of benefits and trade-offs. When faced with the choice of using different approaches to produce a functional MMAM part, the architectures, their tolerance, and the ink rheology must be carefully considered. Inverse design of a process to produce an architecture requires accurate predictions of flow as a function of multiphase rheology, interfacial rheology, flow instabilities, and stability regimes. To build an MMAM architecture using these innovations, the geometry of the nozzle must be planned in conjunction with the print path. The nozzles unlock new handles for architecture design but can also overwhelmingly expand the design space. For this challenge, machine learning may accelerate screening and identification of designs that build suitable architectures while minimizing material waste and internal dead volumes. When new nozzle geometries are designed, assessing their adaptability to inks with rheologies different from those of the original application will be important. In an ideal distributed manufacturing economy, distributed users would have only a few pieces of capital equipment (i.e., nozzles) that they could use with different types of material chemistries.

Fortunately, the 3D-printing community does not start from scratch to work toward this lofty goal. Hard-won knowledge and strategies have been developed in mature fields such as static mixing, manufacturing, and polymer processing to produce parts at capacities that far exceed benchtop 3D printers. Indeed, prior work in these fields expedited the development of all of the nozzle innovations discussed here. By marrying the most advanced iterations of mature technologies within these existing and new arenas, we can undoubtedly extend the capabilities of MMAM.

AUTHOR INFORMATION

Corresponding Author

Alexandra V. Bayles − *Department of Chemical & Biomolecular Engineering, University of Delaware, Newark, Delaware 19716, United States;* orcid.org/0000-0001-9689-9361; Email: avbayles@udel.edu

Author

Patrick J. McCauley − *Department of Chemical & Biomolecular Engineering, University of Delaware, Newark, Delaware 19716, United States;* orcid.org/0000-0003-4168-8983

Complete contact information is available at: https://pubs.acs.org/10.1021/acsengineeringau.4c00001

Author Contributions

CRediT: **Patrick J. McCauley** formal analysis, investigation, methodology, resources, visualization, writing-original draft, writing-review & editing; **Alexandra V. Bayles** conceptualization, funding acquisition, project administration, resources, supervision, writing-original draft, writing-review & editing.

Notes

The authors declare no competing financial interest.

ACKNOWLEDGMENTS

This work was primarily supported by the University of Delaware Startup Funds and the University of Delaware's Institute for Engineering-Driven Health Postdoctoral Fellowship. Partial support was provided by the National Science Foundation (CBET 2339472). Portions of Figures 1, 2, 3, and 5 and the graphical abstract were created with BioRender. Any opinions, findings, and conclusions or recommendations expressed in this material are those of the authors and do not necessarily reflect the views of the National Science Foundation.

REFERENCES

(1) Alessandria, G.; Khan, S. Y.; Khederlarian, A.; Mix, C.; Ruhl, K. J. The aggregate effects of global and local supply chain disruptions: 2020−2022. *J. Int. Econ.* **2023**, *146*, 103788.

(2) Katsaliaki, K.; Galetsi, P.; Kumar, S. Supply chain disruptions and resilience: a major review and future research agenda. *Ann. Oper. Res.* **2022**, *319*, 965−1002.
(3) Llaguno, A.; Mula, J.; Campuzano-Bolarin, F. State of the art, conceptual framework and simulation analysis of the ripple effect on supply chains. *Int. J. Prod. Res.* **2022**, *60*, 2044−2066.
(4) Naghshineh, B.; Carvalho, H. The implications of additive manufacturing technology adoption for supply chain resilience: A systematic search and review. *Int. J. Prod. Econ.* **2022**, *247*, 108387.
(5) Foshammer, J.; Søberg, P. V.; Helo, P.; Ituarte, I. F. Identification of aftermarket and legacy parts suitable for additive manufacturing: A knowledge management-based approach. *Int. J. Prod. Econ.* **2022**, *253*, 108573.
(6) Ekren, B. Y.; Stylos, N.; Zwiegelaar, J.; Turhanlar, E. E.; Kumar, V. Additive manufacturing integration in E-commerce supply chain network to improve resilience and competitiveness. *Simul. Modell. Pract. Theory* **2023**, *122*, 102676.
(7) Afshari, H.; Searcy, C.; Jaber, M. Y. The role of eco-innovation drivers in promoting additive manufacturing in supply chains. *Int. J. Prod. Econ.* **2020**, *223*, 107538.
(8) Gibson, I.; Rosen, D.; Stucker, B.; Khorasani, M. *Additive Manufacturing Technologies: 3D Printing, Rapid Prototyping, and Direct Digital Manufacturing*; Springer, 2021.
(9) Hague, R.; Mansour, S.; Saleh, N. Material and design considerations for Rapid Manufacturing. *Int. J. Prod. Res.* **2004**, *42*, 4691−4708.
(10) Rosen, D.; Kim, S. *Design and Manufacturing Implications of Additive Manufacturing*; ASM International, 2020; pp 19−29.
(11) Thompson, M. K.; Moroni, G.; Vaneker, T.; Fadel, G.; Campbell, R. I.; Gibson, I.; Bernard, A.; Schulz, J.; Graf, P.; Ahuja, B.; Martina, F. others Design for Additive Manufacturing: Trends, opportunities, considerations, and constraints. *CIRP Ann.* **2016**, *65*, 737−760.
(12) Zhang, M.; Yu, Q.; Liu, Z.; Zhang, J.; Tan, G.; Jiao, D.; Zhu, W.; Li, S.; Zhang, Z.; Yang, R.; Ritchie, R. O. 3D printed Mg-NiTi interpenetrating-phase composites with high strength, damping capacity, and energy absorption efficiency. *Sci. Adv.* **2020**, *6*, eaba5581.
(13) Moore, D. G.; Barbera, L.; Masania, K.; Studart, A. R. Three-dimensional printing of multicomponent glasses using phase-separating resins. *Nat. Mater.* **2020**, *19*, 212−217.
(14) Kokkinis, D.; Schaffner, M.; Studart, A. R. Multimaterial magnetically assisted 3D printing of composite materials. *Nat. Commun.* **2015**, *6*, 8643.
(15) Gordeev, E. G.; Galushko, A. S.; Ananikov, V. P. Improvement of quality of 3D printed objects by elimination of microscopic structural defects in fused deposition modeling. *PLoS One* **2018**, *13*, No. e0198370.
(16) Han, D.; Lee, H. Recent advances in multi-material additive manufacturing: methods and applications. *Curr. Opin. Chem. Eng.* **2020**, *28*, 158−166.
(17) Tan, H. W.; An, J.; Chua, C. K.; Tran, T. Metallic Nanoparticle Inks for 3D Printing of Electronics. *Adv. Electron. Mater.* **2019**, *5*, 1800831.
(18) Tan, H. W.; Choong, Y. Y. C.; Kuo, C. N.; Low, H. Y.; Chua, C. K. 3D printed electronics: Processes, materials and future trends. *Prog. Mater. Sci.* **2022**, *127*, 100945.
(19) Pati, F.; Jang, J.; Ha, D.-H.; Kim, S. W.; Rhie, J.-W.; Shim, J.-H.; Kim, D.-H.; Cho, D.-W. Printing three-dimensional tissue analogues with decellularized extracellular matrix bioink. *Nat. Commun.* **2014**, *5*, 3935.
(20) Kolesky, D. B.; Truby, R. L.; Gladman, A. S.; Busbee, T. A.; Homan, K. A.; Lewis, J. A. 3D Bioprinting of Vascularized, Heterogeneous Cell-Laden Tissue Constructs. *Adv. Mater.* **2014**, *26*, 3124−3130.
(21) Peng, F.; Jiang, H.; Woods, A.; Joo, P.; Amis, E. J.; Zacharia, N. S.; Vogt, B. D. 3D Printing with Core-Shell Filaments Containing High or Low Density Polyethylene Shells. *ACS Appl. Polym. Mater.* **2019**, *1*, 275−285.
(22) Naqi, A.; Swain, Z.; Mackay, M. E. Dual Material Fused Filament Fabrication via Core-Shell Die Design. *ACS Appl. Polym. Mater.* **2023**, *5*, 2481−2489.
(23) Bandyopadhyay, A.; Heer, B. Additive manufacturing of multi-material structures. *Mater. Sci. Eng., R* **2018**, *129*, 1−16.
(24) Nazir, A.; Gokcekaya, O.; Billah, K. M. M.; Ertugrul, O.; Jiang, J.; Sun, J.; Hussain, S. Multi-material additive manufacturing: A systematic review of design, properties, applications, challenges, and 3D printing of materials and cellular metamaterials. *Mater. Des.* **2023**, *226*, 111661.
(25) Rafiee, M.; Farahani, R. D.; Therriault, D. Multi-Material 3D and 4D Printing: A Survey. *Adv. Sci.* **2020**, *7*, 1902307.
(26) Pajonk, A.; Prieto, A.; Blum, U.; Knaack, U. Multi-material additive manufacturing in architecture and construction: A review. *J. Build. Eng.* **2022**, *45*, 103603.
(27) Muguruza, A.; Bo, J. B.; Gómez, A.; Minguella-Canela, J.; Fernandes, J.; Ramos, F.; Xuriguera, E.; Varea, A.; Cirera, A. Development of a multi-material additive manufacturing process for electronic devices. *Procedia Manuf.* **2017**, *13*, 746−753.
(28) Dikyol, C.; Altunbek, M.; Bartolo, P.; Koc, B. Multimaterial bioprinting approaches and their implementations for vascular and vascularized tissues. *Bioprinting* **2021**, *24*, No. e00159.
(29) Li, Y.; Feng, Z.; Hao, L.; Huang, L.; Xin, C.; Wang, Y.; Bilotti, E.; Essa, K.; Zhang, H.; Li, Z.; Yan, F.; Peijs, T. A Review on Functionally Graded Materials and Structures via Additive Manufacturing: From Multi-Scale Design to Versatile Functional Properties. *Adv. Mater. Technol.* **2020**, *5*, 1900981.
(30) García-Collado, A.; Blanco, J. M.; Gupta, M. K.; Dorado-Vicente, R. Advances in polymers based Multi-Material Additive-Manufacturing Techniques: State-of-art review on properties and applications. *Addit. Manuf.* **2022**, *50*, 102577.
(31) Chen, H.; Guo, L.; Zhu, W.; Li, C. Recent Advances in Multi-Material 3D Printing of Functional Ceramic Devices. *Polymers* **2022**, *14*, 4635.
(32) Feenstra, D. R.; Banerjee, R.; Fraser, H. L.; Huang, A.; Molotnikov, A.; Birbilis, N. Critical review of the state of the art in multi-material fabrication via directed energy deposition. *Curr. Opin. Solid State Mater. Sci.* **2021**, *25*, 100924.
(33) Wei, C.; Zhang, Z.; Cheng, D.; Sun, Z.; Zhu, M.; Li, L. An overview of laser-based multiple metallic material additive manufacturing: from macro- to micro-scales. *Int. J. Extreme Manuf.* **2021**, *3*, 012003.
(34) Wei, C.; Li, L. Recent progress and scientific challenges in multi-material additive manufacturing via laser-based powder bed fusion. *Virtual Phys. Prototyping* **2021**, *16*, 347−371.
(35) Sampson, K. L.; Deore, B.; Go, A.; Nayak, M. A.; Orth, A.; Gallerneault, M.; Malenfant, P. R.; Paquet, C. Multimaterial Vat Polymerization Additive Manufacturing. *ACS Appl. Polym. Mater.* **2021**, *3*, 4304−4324.
(36) Matsuzaki, R.; Kanatani, T.; Todoroki, A. Multi-material additive manufacturing of polymers and metals using fused filament fabrication and electroforming. *Addit. Manuf.* **2019**, *29*, 100812.
(37) Malone, E.; Rasa, K.; Cohen, D.; Isaacson, T.; Lashley, H.; Lipson, H. Freeform fabrication of zinc-air batteries and electro-mechanical assemblies. *Rapid Prototyping J.* **2004**, *10*, 58−69.
(38) Cohen, D. L.; Malone, E.; Lipson, H.; Bonassar, L. J. Direct freeform fabrication of seeded hydrogels in arbitrary geometries. *Tissue Eng.* **2006**, *12*, 1325−1335.
(39) Haghiashtiani, G.; Habtour, E.; Park, S. H.; Gardea, F.; McAlpine, M. C. 3D printed electrically-driven soft actuators. *Extreme Mech. Lett.* **2018**, *21*, 1−8.
(40) Park, J. H.; El Atrache, A.; Kim, D.; Divo, E. Optimization of helical dielectric elastomer actuator with additive manufacturing. *Proc. SPIE* **2018**, *10594*, 105940Z.
(41) Chortos, A.; Hajiesmaili, E.; Morales, J.; Clarke, D. R.; Lewis, J. A. 3D Printing of Interdigitated Dielectric Elastomer Actuators. *Adv. Funct. Mater.* **2020**, *30*, 1907375.
(42) Danner, P. M.; Pleij, T.; Siqueira, G.; Bayles, A. V.; Venkatesan, T. R.; Vermant, J.; Opris, D. M. Polysiloxane Inks for Multimaterial

3d Printing of High-Permittivity Dielectric Elastomers. *Adv. Funct. Mater.* **2024**, *34*, 2313167.
(43) Kang, H. W.; Lee, S. J.; Ko, I. K.; Kengla, C.; Yoo, J. J.; Atala, A. A 3D bioprinting system to produce human-scale tissue constructs with structural integrity. *Nat. Biotechnol.* **2016**, *34*, 312−319.
(44) Ravichandran, D.; Xu, W.; Kakarla, M.; Jambhulkar, S.; Zhu, Y.; Song, K. Multiphase direct ink writing (MDIW) for multilayered polymer/nanoparticle composites. *Addit. Manuf.* **2021**, *47*, 102322.
(45) Boley, J. W.; van Rees, W. M.; Lissandrello, C.; Horenstein, M. N.; Truby, R. L.; Kotikian, A.; Lewis, J. A.; Mahadevan, L. Shape-shifting structured lattices via multimaterial 4D printing. *Proc. Natl. Acad. Sci. U.S.A.* **2019**, *116*, 20856−20862.
(46) Skylar-Scott, M. A.; Mueller, J.; Visser, C. W.; Lewis, J. A. Voxelated soft matter via multimaterial multinozzle 3D printing. *Nature* **2019**, *575*, 330−335.
(47) National Academy of Engineering and National Academies of Sciences, Engineering, and Medicine. *New Directions for Chemical Engineering*; The National Academies Press: Washington, DC, 2022.
(48) Biedermann, M.; Meboldt, M. Computational design synthesis of additive manufactured multi-flow nozzles. *Addit. Manuf.* **2020**, *35*, 101231.
(49) Meijer, H. E.; Singh, M. K.; Anderson, P. D. On the performance of static mixers: A quantitative comparison. *Prog. Polym. Sci.* **2012**, *37*, 1333−1349.
(50) Neerincx, P. E.; Meijer, H. E. Fractal Structuring in Polymer Processing. *Macromol. Chem. Phys.* **2013**, *214*, 188−202.
(51) Lewis, J. A. Direct ink writing of 3D functional materials. *Adv. Funct. Mater.* **2006**, *16*, 2193−2204.
(52) Frutiger, A.; et al. Capacitive Soft Strain Sensors via Multicore−Shell Fiber Printing. *Adv. Mater.* **2015**, *27*, 2440−2446.
(53) Liu, W.; Zhong, Z.; Hu, N.; Zhou, Y.; Maggio, L.; Miri, A. K.; Fragasso, A.; Jin, X.; Khademhosseini, A.; Zhang, Y. S. Coaxial extrusion bioprinting of 3D microfibrous constructs with cell-favorable gelatin methacryloyl microenvironments. *Biofabrication* **2018**, *10*, 024102.
(54) Hassan, I.; Selvaganapathy, P. R. A microfluidic printhead with integrated hybrid mixing by sequential injection for multimaterial 3D printing. *Addit. Manuf.* **2022**, *50*, 102559.
(55) Chávez-Madero, C.; et al. Using chaotic advection for facile high-throughput fabrication of ordered multilayer micro- and nanostructures: continuous chaotic printing. *Biofabrication* **2020**, *12*, 035023.
(56) Bolívar-Monsalve, E. J.; Ceballos-González, C. F.; Borrayo-Montaño, K. I.; Quevedo-Moreno, D. A.; Yee-de León, J. F.; Khademhosseini, A.; Weiss, P. S.; Alvarez, M. M.; Trujillo-de Santiago, G. Continuous chaotic bioprinting of skeletal muscle-like constructs. *Bioprinting* **2021**, *21*, No. e00125.
(57) Bayles, A. V.; Pleij, T.; Hofmann, M.; Hauf, F.; Tervoort, T.; Vermant, J. Structuring Hydrogel Cross-Link Density Using Hierarchical Filament 3D Printing. *ACS Appl. Mater. Interfaces* **2022**, *14*, 15667−15677.
(58) Pleij, T.; Bayles, A. V.; Vermant, J. Advective Assembler-Enhanced Support Bath Rotational Direct Ink Writing. *Adv. Mater. Technol.* **2024**, DOI: 10.1002/admt.202400005.
(59) Hansen, C. J.; Saksena, R.; Kolesky, D. B.; Vericella, J. J.; Kranz, S. J.; Muldowney, G. P.; Christensen, K. T.; Lewis, J. A. High-throughput printing via microvascular multinozzle arrays. *Adv. Mater.* **2013**, *25*, 96−102.
(60) Hardin, J. O.; Ober, T. J.; Valentine, A. D.; Lewis, J. A. Microfluidic printheads for multimaterial 3D printing of viscoelastic inks. *Adv. Mater.* **2015**, *27*, 3279−3284.
(61) Liu, W.; Zhang, Y. S.; Heinrich, M. A.; De Ferrari, F.; Jang, H. L.; Bakht, S. M.; Alvarez, M. M.; Yang, J.; Li, Y.-C.; Trujillo-de Santiago, G.; et al. Rapid continuous multimaterial extrusion bioprinting. *Adv. Mater.* **2017**, *29*, 1604630.
(62) Timoshenko, S. Analysis of bi-metal thermostats. *J. Opt. Soc. Am.* **1925**, *11*, 233−255.
(63) Sydney Gladman, A.; Matsumoto, E. A.; Nuzzo, R. G.; Mahadevan, L.; Lewis, J. A. Biomimetic 4D printing. *Nat. Mater.* **2016**, *15*, 413−418.
(64) Larson, N. M.; Mueller, J.; Chortos, A.; Davidson, Z. S.; Clarke, D. R.; Lewis, J. A. Rotational multimaterial printing of filaments with subvoxel control. *Nature* **2023**, *613*, 682−688.
(65) Schrenk, W.; Alfrey, T. Coextruded Multilayer Polymer Films and Sheets. *Polym. Blends* **1978**, 129−165.
(66) Djordjevic, D. *Coextrusion*; RAPRA Technology Limited: Shawbury, U.K., 1992.
(67) Peng, F.; Zhao, Z.; Xia, X.; Cakmak, M.; Vogt, B. D. Enhanced Impact Resistance of Three-Dimensional-Printed Parts with Structured Filaments. *ACS Appl. Mater. Interfaces* **2018**, *10*, 16087−16094.
(68) Zhang, G.; Lee, P. C.; Jenkins, S.; Dooley, J.; Baer, E. The effect of confined crystallization on high-density poly(ethylene) lamellar morphology. *Polymer* **2014**, *55*, 663−672.
(69) Richard, C.; Neild, A.; Cadarso, V. J. The emerging role of microfluidics in multi-material 3D bioprinting. *Lab Chip* **2020**, *20*, 2044−2056.
(70) Mea, H.; Wan, J. Microfluidics-enabled functional 3D printing. *Biomicrofluidics* **2022**, *16*, 021501.
(71) Ibrahim, Y.; Elkholy, A.; Schofield, J. S.; Melenka, G. W.; Kempers, R. Effective thermal conductivity of 3D-printed continuous fiber polymer composites. *Adv. Manuf.: Polym. Compos. Sci.* **2020**, *6*, 17−28.
(72) Zhang, Y.; Yu, Y.; Akkouch, A.; Dababneh, A.; Dolati, F.; Ozbolat, I. T. In vitro study of directly bioprinted perfusable vasculature conduits. *Biomater. Science* **2015**, *3*, 134−143.
(73) Yu, Y.; Zhang, Y.; Martin, J. A.; Ozbolat, I. T. Evaluation of cell viability and functionality in vessel-like bioprintable cell-laden tubular channels. *J. Biomech. Eng.* **2013**, *135*, 091011.
(74) Shao, L.; Gao, Q.; Xie, C.; Fu, J.; Xiang, M.; He, Y. Directly coaxial 3D bioprinting of large-scale vascularized tissue constructs. *Biofabrication* **2020**, *12*, 035014.
(75) Akkineni, A. R.; Ahlfeld, T.; Lode, A.; Gelinsky, M. A versatile method for combining different biopolymers in a core/shell fashion by 3D plotting to achieve mechanically robust constructs. *Biofabrication* **2016**, *8*, 045001.
(76) Ai, J. R.; Peng, F.; Joo, P.; Vogt, B. D. Enhanced Dimensional Accuracy of Material Extrusion 3D-Printed Plastics through Filament Architecture. *ACS Appl. Polym. Mater.* **2021**, *3*, 2518−2528.
(77) Tran, T. Q.; Ng, F. L.; Kai, J. T. Y.; Feih, S.; Nai, M. L. S. Tensile Strength Enhancement of Fused Filament Fabrication Printed Parts: A Review of Process Improvement Approaches and Respective Impact. *Addit. Manuf.* **2022**, *54*, 102724.
(78) Gao, X.; Qi, S.; Kuang, X.; Su, Y.; Li, J.; Wang, D. Fused filament fabrication of polymer materials: A review of interlayer bond. *Addit. Manuf.* **2021**, *37*, 101658.
(79) Goh, G. D.; Yap, Y. L.; Tan, H. K.; Sing, S. L.; Goh, G. L.; Yeong, W. Y. Process−Structure−Properties in Polymer Additive Manufacturing via Material Extrusion: A Review. *Crit. Rev. Solid State Mater. Sci.* **2020**, *45*, 113−133.
(80) Koker, B.; Ruckdashel, R.; Abajorga, H.; Curcuru, N.; Pugatch, M.; Dunn, R.; Kazmer, D. O.; Wetzel, E. D.; Park, J. H. Enhanced interlayer strength and thermal stability via dual material filament for material extrusion additive manufacturing. *Addit. Manuf.* **2022**, *55*, 102807.
(81) Galaktionov, O. S.; Anderson, P. D.; Peters, G. W.; Meijer, H. E. Analysis and optimization of Kenics static mixers. *Int. Polym. Process.* **2003**, *18*, 138−150.
(82) Singh, M. K.; Anderson, P. D.; Meijer, H. E. H. Understanding and Optimizing the SMX Static Mixer. *Macromol. Rapid Commun.* **2009**, *30*, 362−376.
(83) Meijer, H. E.; Janssen, J. M.; Anderson, P. D. Mixing of immiscible liquids. In *Mixing and Compounding of Polymers: Theory and Practice*; Hanser Publications, 1994; pp 85−148.
(84) Godfrey, J. Static Mixers. In *Mixing in the Process Industries*; Butterworth-Heinemann: Oxford, U.K., 1992.

(85) Valdés, J. P.; Kahouadji, L.; Matar, O. K. Current advances in liquid−liquid mixing in static mixers: A review. *Chem. Eng. Res. Des.* **2022**, *177*, 694−731.
(86) Simpson, T. A.; Dawson, M. K.; Etchellsi, A. Update to Mixing in Pipelines. In *Advances in Industrial Mixing*; Kresta, S. M., et al., Eds.; Wiley: Hoboken, NJ, 2015; Chapter 7b, pp 205−237.
(87) Chen, H.; Meiners, J. C. Topologic mixing on a microfluidic chip. *Appl. Phys. Lett.* **2004**, *84*, 2193−2195.
(88) Kim, D. S.; Lee, S. H.; Kwon, T. H.; Ahn, C. H. A serpentine laminating micromixer combining splitting/recombination and advection. *Lab Chip* **2005**, *5*, 739−747.
(89) Kang, T. G.; Singh, M. K.; Anderson, P. D.; Meijer, H. E. A chaotic serpentine mixer efficient in the creeping flow regime: From design concept to optimization. *Microfluid. Nanofluid.* **2009**, *7*, 783.
(90) Ponting, M.; Hiltner, A.; Baer, E. Polymer nanostructures by forced assembly: Process, structure, and properties. *Macromol. Symp.* **2010**, *294*, 19−32.
(91) Neerincx, P. E.; Denteneer, R. P.; Peelen, S.; Meijer, H. E. Compact mixing using multiple splitting, stretching, and recombining flows. *Macromol. Mater. Eng.* **2011**, *296*, 349−361.
(92) Li, Z.; Olah, A.; Baer, E. Micro- and nano-layered processing of new polymeric systems. *Prog. Polym. Sci.* **2020**, *102*, 101210.
(93) Langhe, D.; Ponting, M. *Manufacturing and Novel Applications of Multilayer Polymer Films*; William Andrew Publishing: Norwich, NY, 2016.
(94) Schaller, R.; Neerincx, P. E.; Meijer, H. E. Hierarchical and Fractal Structuring in Polymer Processing. *Macromol. Mater. Eng.* **2017**, *302*, 1600524.
(95) Kruijt, P. G. M.; Galaktionov, O. S.; Peters, G. W. M.; Meijer, H. E. H. The Mapping Method for Mixing Optimization. *Int. Polym. Process.* **2001**, *16*, 161−171.
(96) Sluijters, R. Mixing Apparatus. US 3051453, 1962.
(97) Mueller, C. D.; Nazarenko, S.; Ebeling, T.; Schuman, T. L.; Hiltner, A.; Baer, E. Novel structures by microlayer coextrusion - Talc-filled PP, PC/SAN, and HDPE/LLDPE. *Polym. Eng. Sci.* **1997**, *37*, 355−362.
(98) Wang, H.; Keum, J. K.; Hiltner, A.; Baer, E. Confined crystallization of peo in nanolayered films impacting structure and oxygen permeability. *Macromolecules* **2009**, *42*, 7055−7066.
(99) Wang, H.; Keum, J. K.; Hiltner, A.; Baer, E.; Freeman, B.; Rozanski, A.; Galeski, A. Confined crystallization of polyethylene oxide in nanolayer assemblies. *Science* **2009**, *323*, 757−760.
(100) Ponting, M.; Lin, Y.; Keum, J. K.; Hiltner, A.; Baer, E. Effect of substrate on the isothermal crystallization kinetics of confined poly(caprolactone) nanolayers. *Macromolecules* **2010**, *43*, 8619−8627.
(101) Carr, J. M.; Langhe, D. S.; Ponting, M. T.; Hiltner, A.; Baer, E. Confined crystallization in polymer nanolayered films: A review. *J. Mater. Res.* **2012**, *27*, 1326−1350.
(102) Kazmierczak, T.; Song, H.; Hiltner, A.; Baer, E. Polymeric One-Dimensional Photonic Crystals by Continuous Coextrusion. *Macromol. Rapid Commun.* **2007**, *28*, 2210−2216.
(103) Ponting, M.; Burt, T. M.; Korley, L. T.; Andrews, J.; Hiltner, A.; Baer, E. Gradient multilayer films by forced assembly coextrusion. *Ind. Eng. Chem. Res.* **2010**, *49*, 12111−12118.
(104) Miriyev, A.; Xia, B.; Joseph, J. C.; Lipson, H. Additive manufacturing of silicone composites for soft actuation. *3D Printing Addit. Manuf.* **2019**, *6*, 309−318.
(105) Gharaie, S.; Zolfagharian, A.; Moghadam, A. A. A.; Shukur, N.; Bodaghi, M.; Mosadegh, B.; Kouzani, A. Direct 3D printing of a two-part silicone resin to fabricate highly stretchable structures. *Prog. Addit. Manuf.* **2023**, *8*, 1555−1571.
(106) Idaszek, J.; et al. 3D bioprinting of hydrogel constructs with cell and material gradients for the regeneration of full-thickness chondral defect using a microfluidic printing head. *Biofabrication* **2019**, *11*, 044101.
(107) Bakarich, S. E.; Gorkin, R.; Gately, R.; Naficy, S.; in het Panhuis, M.; Spinks, G. M. 3D printing of tough hydrogel composites with spatially varying materials properties. *Addit. Manuf.* **2017**, *14*, 24−30.
(108) Guo, W.; Jiang, Z.; Zhong, H.; Chen, G.; li, X.; Yan, H.; Zhang, C.; Zhao, L. others 3D printing of multifunctional gradient bone scaffolds with programmable component distribution and hierarchical pore structure. *Composites, Part A* **2023**, *166*, 107361.
(109) Wegst, U. G.; Bai, H.; Saiz, E.; Tomsia, A. P.; Ritchie, R. O. Bioinspired structural materials. *Nat. Mater.* **2015**, *14*, 23−36.
(110) Seidi, A.; Ramalingam, M.; Elloumi-Hannachi, I.; Ostrovidov, S.; Khademhosseini, A. Gradient biomaterials for soft-to-hard interface tissue engineering. *Acta Biomater.* **2011**, *7*, 1441−1451.
(111) Kokkinis, D.; Bouville, F.; Studart, A. R. 3D printing of materials with tunable failure via bioinspired mechanical gradients. *Adv. Mater.* **2018**, *30*, 1705808.
(112) Sola, A.; Bellucci, D.; Cannillo, V. Functionally graded materials for orthopedic applications − an update on design and manufacturing. *Biotechnol. Adv.* **2016**, *34*, 504−531.
(113) Wang, P.; Sun, Y.; Ma, Z.; Diao, L.; Liu, H.; Shastri, V. P. Novel stirring-rod-inspired mixer-integrated printhead for fabricating gradient tissue structures. *Mater. Des.* **2023**, *229*, 111866.
(114) Bolívar-Monsalve, E. J.; Ceballos-González, C. F.; Chávez-Madero, C.; de la Cruz-Rivas, B. G.; Velásquez Marín, S.; Mora-Godínez, S.; Reyes-Cortés, L. M.; Khademhosseini, A.; Weiss, P. S.; Samandari, M.; Tamayol, A.; Alvarez, M. M.; Trujillo-de Santiago, G.; et al. One-Step Bioprinting of Multi-Channel Hydrogel Filaments Using Chaotic Advection: Fabrication of Pre-Vascularized Muscle-Like Tissues. *Adv. Healthcare Mater.* **2022**, *11*, 2200448.
(115) Jambhulkar, S.; Ravichandran, D.; Thippanna, V.; Patil, D.; Song, K. A multimaterial 3D printing-assisted micropatterning for heat dissipation applications. *Adv. Compos. Hybrid Mater.* **2023**, *6*, 93.
(116) Chang, R.; Nam, J.; Sun, W. Effects of Dispensing Pressure and Nozzle Diameter on Cell Survival from Solid Freeform Fabrication−Based Direct Cell Writing. *Tissue Eng., Part A* **2008**, *14*, 41−48.
(117) Boularaoui, S.; Al Hussein, G.; Khan, K. A.; Christoforou, N.; Stefanini, C. An overview of extrusion-based bioprinting with a focus on induced shear stress and its effect on cell viability. *Bioprinting* **2020**, *20*, No. e00093.
(118) Zhang, B.; Gao, L.; Gu, L.; Yang, H.; Luo, Y.; Ma, L. High-resolution 3D Bioprinting System for Fabricating Cell-laden Hydrogel Scaffolds with High Cellular Activities. *Procedia CIRP* **2017**, *65*, 219−224.
(119) Karvinen, J.; Kellomäki, M. Design aspects and characterization of hydrogel-based bioinks for extrusion-based bioprinting. *Bioprinting* **2023**, *32*, No. e00274.
(120) Ceballos-González, C. F.; Bolívar-Monsalve, E. J.; Quevedo-Moreno, D. A.; Lam-Aguilar, L. L.; Borrayo-Montaño, K. I.; Yee-de León, J. F.; Zhang, Y. S.; Alvarez, M. M.; Trujillo-de Santiago, G. High-Throughput and Continuous Chaotic Bioprinting of Spatially Controlled Bacterial Microcosms. *ACS Biomater. Sci. Eng.* **2021**, *7*, 2408−2419.
(121) Cui, H.; Zhu, W.; Huang, Y.; Liu, C.; Yu, Z. X.; Nowicki, M.; Miao, S.; Cheng, Y.; Zhou, X.; Lee, S. J.; Zhou, Y.; Wang, S.; Mohiuddin, M.; Horvath, K.; Zhang, L. G. In vitro and in vivo evaluation of 3D bioprinted small-diameter vasculature with smooth muscle and endothelium. *Biofabrication* **2020**, *12*, 015004.
(122) Jain, R. K.; Au, P.; Tam, J.; Duda, D. G.; Fukumura, D. Engineering vascularized tissue. *Nat. Biotechnol.* **2005**, *23*, 821−823.
(123) Ceballos-González, C. F.; Bolívar-Monsalve, E. J.; Quevedo-Moreno, D. A.; Chávez-Madero, C.; Velásquez-Marín, S.; Lam-Aguilar, L. L.; Solís-Pérez, Ó. E.; Cantoral-Sánchez, A.; Neher, M.; Yzar-García, E.; Zhang, Y. S.; Gentile, C.; Boccaccini, A. R.; Alvarez, M. M.; Trujillo-de Santiago, G. Plug-and-Play Multimaterial Chaotic Printing/Bioprinting to Produce Radial and Axial Micropatterns in Hydrogel Filaments. *Adv. Mater. Technol.* **2023**, *8*, 2202208.
(124) Ravichandran, D.; Ahmed, R. J.; Banerjee, R.; Ilami, M.; Marvi, H.; Miquelard-Garnier, G.; Golan, Y.; Song, K. Multi-material 3D printing-enabled multilayers for smart actuation via magnetic and thermal stimuli. *J. Mater. Chem. C* **2022**, *10*, 13762−13770.
(125) Ravichandran, D.; Kakarla, M.; Xu, W.; Jambhulkar, S.; Zhu, Y.; Bawareth, M.; Fonseca, N.; Patil, D.; Song, K. 3D-printed in-line

and out-of-plane layers with stimuli-responsive intelligence. *Composites, Part B* **2022**, *247*, 110352.
(126) Barad, H. N.; Kwon, H.; Alarcón-Correa, M.; Fischer, P. Large Area Patterning of Nanoparticles and Nanostructures: Current Status and Future Prospects. *ACS Nano* **2021**, *15*, 5861−5875.
(127) Bayles, A. V.; Vermant, J. Divide, conquer, and stabilize: Engineering strong fluid−fluid interfaces. *Langmuir* **2022**, *38*, 6499−6505.
(128) Neerincx, P. E.; Hofmann, M.; Gorodetskyi, O.; Feldman, K.; Vermant, J.; Meijer, H. E. H. One-step creation of hierarchical fractal structures. *Polym. Eng. Sci.* **2021**, *61*, 1257−1269.
(129) Hofmann, M.; Bayles, A. V.; Vermant, J. Stretch, fold, and break: Intensification of emulsification of high viscosity ratio systems by fractal mixers. *AIChE J.* **2021**, *67*, No. e17192.
(130) Hooghten, R. V.; Hofmann, M.; Vermant, J. Method for producing emulsions and aqueous polyisobutene emulsion. US 20210340335 A1, 2021.
(131) Bayles, A. V.; Hofmann, M.; Vermant, J. Method for producing emulsions. US 20230172252 A1, 2023.
(132) Möller, A. C.; van der Goot, A. J.; van der Padt, A. A novel process to produce stratified structures in food. *J. Food Eng.* **2023**, *345*, 111413.
(133) Le, X.; Lu, W.; Zhang, J.; Chen, T. Recent Progress in Biomimetic Anisotropic Hydrogel Actuators. *Adv. Sci.* **2019**, *6*, 1801584.
(134) Yih, C.-S. Instability due to viscosity stratification. *J. Fluid Mech.* **1967**, *27*, 337−352.
(135) Lamnawar, K.; Bousmina, M.; Maazouz, A. 2D encapsulation in multiphase polymers: Role of viscoelastic, geometrical and interfacial properties. *Macromolecules* **2012**, *45*, 441−454.
(136) Anderson, P. D.; Dooley, J.; Meijer, H. E. H. Viscoelastic effects in multilayer polymer extrusion. *Appl. Rheol.* **2006**, *16*, 198−205.
(137) Van Der Hoeven, J. C.; Wimberger-Friedl, R.; Meijer, H. E. Homogeneity of multilayers produced with a static mixer. *Polym. Eng. Sci.* **2001**, *41*, 32−42.
(138) Harris, P. J.; Patz, J.; Huntington, B. A.; Bonnecaze, R. T.; Meltzer, D.; Maia, J. Improved interfacial surface generator for the coextrusion of micro-and nanolayered polymers. *Polym. Eng. Sci.* **2014**, *54*, 636−645.
(139) Bayles, A. V.; Pleij, T.; Nam, J. E.; Murdock, M. N.; Vermant, J. *Boolean Simulink Package*. https://github.com/Bayles-Research-Group (accessed 2023-12-30).

https://doi.org/10.1021/acsengineeringau.4c00001
ACS Eng. Au 2024, 4, 368−380